Thermal formation of hydroxynitriles, precursors of hydroxyacids in astrophysical ice analogs: acetone ((CH3)2C=O) and hydrogen cyanide (HCN) reactivity

Aurelien Fresneau, Grégoire Danger, Albert Rimola, Fabrice Duvernay, Patrice Theulé, Thierry Chiavassa

Thermal formation of hydroxynitriles, precursors of hydroxyacids in astrophysical ice analogs: Acetone ((CH3)2CO) and...

Article · November 2015

DOI: 10.1016/j.molap.2015.10.001

CITATIONS
0

READS
72

6 authors, including:

Grégoire Danger
Aix-Marseille Université
80 PUBLICATIONS **720** CITATIONS
SEE PROFILE

Albert Rimola
Autonomous University of Barcelona
70 PUBLICATIONS **1,345** CITATIONS
SEE PROFILE

F. Duvernay
Aix-Marseille Université
62 PUBLICATIONS **743** CITATIONS
SEE PROFILE

Patrice Theulé
Aix-Marseille Université
32 PUBLICATIONS **196** CITATIONS
SEE PROFILE

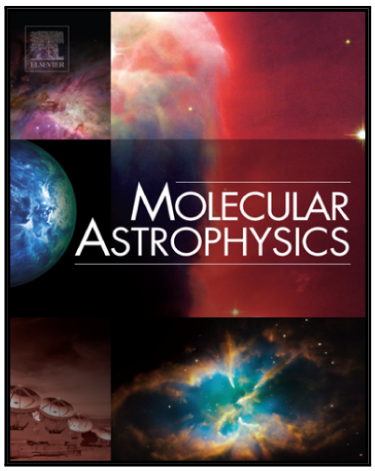

Thermal formation of hydroxynitriles, precursors of hydroxyacids in astrophysical ice analogs: acetone ($(CH_3)_2C{=}O$) and hydrogen cyanide (HCN) reactivity

Aurélien Fresneau , Grégoire Danger , Albert Rimola , Fabrice Duvernay , Patrice Theulé , Thierry Chiavassa

PII: S2405-6758(15)30004-X
DOI: 10.1016/j.molap.2015.10.001
Reference: MOLAP 4

To appear in: *Molecular Astrophysics*

Received date: 23 June 2015
Revised date: 26 October 2015

Please cite this article as: Aurélien Fresneau , Grégoire Danger , Albert Rimola , Fabrice Duvernay , Patrice Theulé , Thierry Chiavassa , Thermal formation of hydroxynitriles, precursors of hydroxyacids in astrophysical ice analogs: acetone ($(CH_3)_2C{=}O$) and hydrogen cyanide (HCN) reactivity, *Molecular Astrophysics* (2015), doi: 10.1016/j.molap.2015.10.001

Thermal formation of hydroxynitriles, precursors of hydroxyacids in astrophysical ice analogs: acetone ($(CH_3)_2C=O$) and hydrogen cyanide (HCN) reactivity

Aurélien Fresneau[a], Grégoire Danger[*a], Albert Rimola[*b], Fabrice Duvernay[a], Patrice Theulé[a] and Thierry Chiavassa[a]

[a]*Aix-Marseille Université, PIIM UMR-CNRS 7345, F-13397 Marseille, France, *E-mail: gregoire.danger@univ-amu.fr*
[b]*Departament de Química, Universitat Autònoma de Barcelona, 08193, Bellaterra, Spain, *E-mail: albert.rimola@uab.cat*

Abstract

Reactivity in astrophysical environments is still poorly understood. In this contribution, we investigate the thermal reactivity of interstellar ice analogs containing acetone ($(CH_3)_2CO$), ammonia (NH_3), hydrogen cyanide (HCN) and water (H_2O) by means of infrared spectroscopy and mass spectrometry techniques, complemented by quantum chemical calculations. We show that no reaction occurs in H_2O:HCN:$(CH_3)_2CO$ ices. Nevertheless, HCN does indeed react with acetone once activated by NH_3 into CN^- to form 2-hydroxy-2-methylpropanenitrile ($HO\text{-}C(CH_3)_2\text{-}CN$), with a calculated activation energy associated with the rate determining step of about 51 kJ mol^{-1}. This reaction inhibits the formation of 2-aminopropan-2-ol ($HO\text{-}C(CH_3)_2\text{-}NH_2$) from acetone and NH_3, even in the presence of water, which is the first step of the Strecker synthesis to form 2-aminoisobutyric acid ($NH_2C(CH_3)_2COOH$). However, $HO\text{-}C(CH_3)_2\text{-}CN$ formation could be part of an alternative chemical pathway leading to 2-hydroxy-2-methyl-propanoic acid ($HOC(CH_3)_2COOH$), which could explain the presence of hydroxy acids in some meteorites.

1 Introduction

Getting a better understanding of the universality of the formation of complex organic molecules present in the interstellar medium (ISM) and in small bodies such as comets and asteroids is the preliminary step towards prebiotic chemistry on Earth, as those organic molecules coming from exogenous sources may have played a major role in the emergence of life on Earth (Ehrenfreund and Charnley, 2000). Many interstellar molecules are thought to be formed in the gas phase (Herbst and van Dishoeck, 2009), but it is undeniable that solid-phase chemistry on the surface of interstellar grains has a role to play in the synthesis of several complex organic molecules. For instance, when a dense molecular cloud collapses to form a protostar, interstellar grains receive energy - heat and irradiation - and are chemically processed. Those processed grains agglomerate in later stages of the protostellar disk to form planitesimals, comets and asteroids. Thus, complex organic molecules detected in these interplanetary bodies may find their origins in interstellar grains. Among the most interesting organic molecules, amino acids are of paramount relevance from an astrobiology standpoint because they are the building blocks of proteins on Earth. Amino acids have been found in carbonaceous chondrites (Kvenvolden et al., 1970; Cronin and Moore, 1971; Engel and Macko, 1997; Martins et al., 2007; Glavin et al., 2010; Burton et al., 2014), and glycine, the simplest amino acid, has also been detected in the comet 81P/Wild 2 after analyzing samples from the Stardust mission (Elsila et al., 2009).

Several chemical pathways have been proposed to explain the origin of these amino acids. Some require UV irradiation, such as the formation of glycine from methylamine and CO_2 (Bossa, Duvernay, et al., 2009), while

others are only based on thermal processes. The most relevant one is the Strecker synthesis (Strecker, 1854). It envisages the reaction between an aldehyde or a ketone ($R_1R_2C=O$) with ammonia (NH_3) and hydrogen cyanide (HCN) to form first an aminonitrile ($H_2N\text{-}CR_1R_2\text{-}CN$), which can subsequently be hydrated to form an amino acid. The Strecker synthesis is believed to be the main reaction pathway that leads to amino acids in some meteorites (Peltzer and Bada, 1978) because their parent bodies have gone through aqueous alteration of their composition (Rubin et al., 2007; Le Guillou et al., 2014). Several laboratory experiments have been conducted to understand if this reaction can also occur in the bulk of icy mantles of interstellar or cometary grains. Different steps of the Strecker reaction have been considered separately and validated with the help of interstellar ice analogs in the case of formaldehyde (CH_2O) (Bossa, Theulé, et al., 2009; Danger et al., 2011; Vinogradoff, Rimola, et al., 2012), acetaldehyde (CH_3CHO) (Duvernay et al., 2010; Vinogradoff, Duvernay, et al., 2012), and acetone ($(CH_3)_2CO$) (Fresneau et al., 2014). Quantum chemical calculations also addressed the formation of glycine through the Strecker synthesis (Rimola et al., 2010), as well as other radical-based paths (Rimola et al., 2012).

In the first step of the Strecker synthesis, NH_3 reacts with an aldehyde or a ketone to form the corresponding aminoalcohol ($H_2N\text{-}CR_1R_2\text{-}OH$). It was shown that in the case of acetone this first step only occurs in the presence of water, that traps NH_3 and acetone in the solid phase above their desorption temperature, allowing them to react to form 2-aminopropan-2-ol (Fresneau et al., 2014). For formaldehyde and acetaldehyde, the reaction with NH_3 occurs with or without water in the ice. However, if HCN is added to the initial mixture, a competition appears between the formation of the aminoalcohol and the hydroxynitrile ($H_2N\text{-}CR_1R_2\text{-}CN$), which takes place by a nucleophilic attack of CN^- to the aldehyde (Danger et al., 2012; Fresneau et al., 2015).

In this work, by using infrared spectroscopy coupled with mass spectrometry, and complemented by quantum chemical calculations, we study if the same kind of competition to form either 2-aminopropan-2-ol ($H_2N\text{-}C(CH_3)_2\text{-}OH$) or 2-hydroxy-2-methylpropanenitrile ($HO\text{-}C(CH_3)_2\text{-}CN$, also known as acetone cyanohydrin) also occurs within acetone ices containing NH_3, HCN, and/or H_2O. We also discuss the implications of these results for the Strecker synthesis in the solid phase in the case of acetone.

2 Methods

2.1 Experimental set-up and reactant syntheses

Potassium cyanide (KCN), acetone ($(CH_3)_2CO$ (≥99.9%) and 2-hydroxy-2-methylpropanenitrile ($HO\text{-}C(CH_3)_2\text{-}CN$) were purchased from Sigma Aldrich, stearic acid from Fluka analytical, and ammonia (NH_3) (99.9%) from Air Liquide. Water (H_2O) was distilled in the laboratory. The hydrogen cyanide (HCN) gas used in all experiments was synthesized by heating a stoichiometric mixture of KCN and stearic acid in a Pyrex line at 10^{-3} mbar following the protocol described by Gerakines *et al*. (Gerakines et al., 2004).

The high vacuum chamber used for the experiments presents a pressure of 5×10^{-9} mbar at 295 K and 1×10^{-9} mbar at 20 K. The gaseous mixtures prepared in a gas line were deposited at a rate of 1 µmol min^{-1} on a copper surface cooled down to 20 K with a model 21 CTI cold head. We checked that copper does not react with any of the compounds used in this study. The following equation described in (Mispelaer et al., 2013) was used to estimate the thickness of the ices, based on the IR spectra:

$$d_{[an]} \frac{N \times 18}{\rho \times N_A} \times \frac{\cos \alpha}{2}$$

where N is the measured column density (molecules cm^{-2}), N_A is the Avogadro number, 18 g mol^{-1} is the molar mass of H_2O, ρ=0.94 g cm^{-2} is the density of the amorphous ice (Mispelaer et al., 2013) and α is the angle between the IR beam and the surface normal (α=0 in our case). For this calculation, we made the approximation that the ice only contains H_2O – the most abundant species in the ice. This leads to an underestimation of the thickness. In light of these considerations, the thickness of the ices formed varies between 0.2 and 0.6 μm. The ices were then warmed at a rate of 4 K min^{-1} using a resistive heater along with a Lakeshore model 331 temperature controller. The infrared (IR) spectra of the sample were recorded in reflection absorption mode between 4000 and 600 cm^{-1} using a Brucker Tensor 27 FTIR spectrometer with a MCT detector. Each spectrum was averaged over 100 scans with a 1 cm^{-1} resolution. Mass spectra were monitored using a RGA quadrupole mass spectrometer (MKS Microvision-IP plus) as the products desorbed during the controlled warming. The ionization source was a 70 eV impact electronic source and the mass spectra were recorded between 1 and 100 amu in a full scan.

The ratios between H_2O, NH_3, HCN and $(CH_3)_2CO$ in the initial ices have been estimated by using characteristic infrared features of each compound. The following band strengths were used: for HCN $\nu_{C\equiv N}$ at 2083 cm^{-1} with 5.1 × 10^{-18} cm $molecule^{-1}$ (Bernstein et al., 1997), for H_2O ν_{OH} at 3340 cm^{-1} with 2 × 10^{-16} cm $molecule^{-1}$ (Gerakines et al., 1995), for $(CH_3)_2CO$ ν_{CO} at 1704 cm^{-1} with 1 × 10^{-17} cm $molecule^{-1}$, and for NH_3 ω_{NH} at 1109 cm^{-1} 1.3 × 10^{-17} cm $molecule^{-1}$ (Kerkhof et al., 1999). IR bands chosen for quantitative estimations of NH_3, HCN and $(CH_3)_2CO$ do not overlap with bands of other compounds, making calculations straightforward. However, the ν_{OH} stretching mode of H_2O at 3340 cm^{-1} overlaps with features of NH_3 and HCN. The amount of NH_3 and HCN is calculated first, and the corresponding areas are subtracted to the band at 3340 cm^{-1} to estimate the amount of H_2O. A former study (Bouilloud et al., 2015) estimated uncertainties of about 20 percent in the measurements of band strengths for CO_2, CO, CH_4 and NH_3 icy films. It should also be kept in mind that all band strengths used to calculate ratios are that of pure ices. They do not take into account the variation induced by the mixture, possibly leading to more uncertainty.

2.2 Computational details

All calculations were performed using the GAUSSIAN09 package program (Frisch et al., 2013). The structure of each stationary point was fully optimized using the hybrid B3LYP-D3 method, which includes an empirical a posteriori correction term proposed by Grimme (Grimme et al., 2010) to account for dispersion forces (missed in the pure B3LYP functional (Lee et al., 1988; Becke, 1993)) with the standard 6-31+G(d,p) basis set. All structures were characterized by the analytical calculation of the harmonic frequencies as minima (reactants, intermediates and products) and saddle points (transition states). For some difficult cases, intrinsic reaction coordinate (IRC) calculations at the same level of theory were carried out to ensure that a given transition structure connects the expected reactants and products. The free energies calculated at different temperatures were obtained by computing the thermochemical corrections to the energy values using the standard harmonic oscillator formulae (McQuarrie, 1986) computed at B3LYP/6-31+G(d,p).

The theoretical simulation of the infrared spectra of an amorphous ice of $HOC(CH_3)_2CN$ was done in a two-step procedure. The first step was the execution of classical molecular dynamics (MD) simulations of a large cluster model of 36 molecules to obtain a preliminary amorphous structure of the ice. These MD simulations were carried out in a (N,V,T) ensemble at T = 300 K with the MMF94 classical force field as implemented in the ChemBio3D Ultra program. The resulting structure was used to obtain a smaller 3D periodic system consisting

of 9 $HOC(CH_3)_2CN$ molecules in a cubic unit system with an initial length of 10 Å. This periodic system was fully optimized (both internal atomic positions and lattice unit cell parameters) using the CRYSTAL09 code (Dovesi et al., 2009). The final optimized structure of this ice model is shown in Figure 1. This ice was then used to simulate its infrared spectrum. The geometry optimization and the simulation of the infrared spectra was carried out using the B3LYP-D2* density functional with a double-ζ basis set, in which the original D2 Grimme dispersion term (Grimme, 2006) was modified for extended systems (D2*), to provide accurate results for the calculations of cohesive energies of molecular crystals (Civalleri et al., 2008). The vibrational frequencies of the simulated spectra have been scaled by a 0.9627 factor (Merrick et al., 2007).

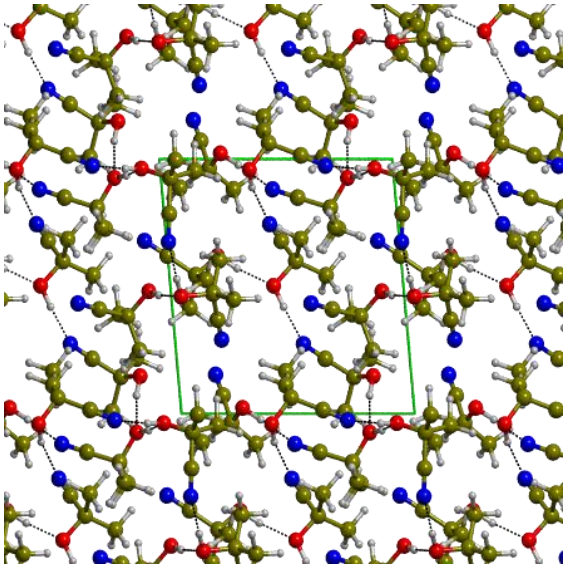

Figure 1: B3LYP-D2*-optimized geometry of a periodic amorphous ice model of $HO\text{-}C(CH_3)_2\text{-}CN$ consisting of 9 molecules per unit cell. The initial lattice parameters (a=b=c= 10.0 Å, and α=β=γ= 90 degrees) upon optimization are a= 10.1899, b= 10.8787 and c= 10.5904 Å, and α= 74.52, β= 88.53 and γ= 94.75 degrees.

3 Results

3.1 NH_3:HCN:$(CH_3)_2CO$ ice reactivity

As stated in the introduction, former studies have shown that aldehydes can react with NH_3 to form the corresponding aminoalcohol, regardless of the presence of H_2O or not. In contrast, the reactivity between ketones and NH_3 is not as straightforward since acetone ($(CH_3)_2CO$) and ammonia (NH_3) react together in the solid phase exclusively in the presence of H_2O (Fresneau et al., 2014), leading to the formation of 2-aminopropan-2-ol ($H_2N\text{-}C(CH_3)_2\text{-}OH$). Aldehydes and HCN alone do not react together. In a similar way, a HCN:$(CH_3)_2CO$ ice shows no reactivity. However, in the presence of H_2O or NH_3, HCN and aldehydes form hydroxynitriles. When NH_3 is added to a HCN:aldehyde ice, there is a competition between the formation of the aminoalcohol and the hydroxynitrile. Here, the same chemical reactivity study is performed with acetone. Mixtures of NH_3:HCN:$(CH_3)_2CO$ containing either $HC^{14}N$ or $HC^{15}N$ were deposited in a 1:0.9:0.6 ratio at 20 K. Their IR spectra are shown in Figure 2A. Apart from the 31 cm^{-1} shift of the $\nu_{C\equiv N}$ from 2083 cm^{-1} for $HC^{14}N$ to 2052 cm^{-1} for $HC^{15}N$, both ices show similar features. All infrared bands attributed to the reactants are reported in Table 1. On top of the signatures of NH_3, HCN and $(CH_3)_2CO$, the band at 1480 cm^{-1} attests the presence of ammonium ions (NH_4^+) in the ice. This means that NH_3 and HCN react to form $[NH_4^+\ ^-CN]$ in the solid phase at

20 K or during the deposition. This has already been observed in previous studies (Danger et al., 2012; Noble et al., 2013; Fresneau et al., 2015). The presence of [NH_4^+ $^-$CN] indicates that both HCN and CN^- contribute to the band at 2083 cm^{-1} (2053 cm^{-1} for $HC^{15}N$), making quantitative estimations less reliable. Upon heating the ice at 4 K min^{-1}, IR bands of reactants decrease and eventually disappear, due to the desorption of the components. However, at 190 K a residue characterized by the IR spectrum displayed in Figure 2B remains, showing that a solid phase reaction occurred during the ice warming. A $\nu_{C\equiv N}$ band shift from 2242 cm^{-1} s to 2211 cm^{-1} for the ice containing $HC^{15}N$ proves that a product with a C≡N moiety was formed. The IR spectrum seems to correspond to hydroxynitrile derivatives (Danger et al., 2012; Danger et al., 2014; Fresneau et al., 2015). By comparing it to the spectrum of hydroxyacetonitrile (HO-CH_2-CN) from Danger *et al.* (Danger et al., 2012), characteristic vibration modes can be assigned to some IR bands: ν_{CO} at 1188 cm^{-1}, δ_{OH} at 1667 cm^{-1}, ν_{CH} asymmetric (a.s.) at 2988 cm^{-1} and symmetric (s.) at 2940 cm^{-1}. All band attributions are summarized in Table 2.

Table 1: Infrared band positions and their attributions to the different reactants in NH_3:HCN:$(CH_3)_2CO$ 1:0.9:0.6 ices at 20 K

Band positions (cm^{-1})					Attributions
acetone	NH_3	HCN	CN^-	NH^{4+}	
-	3386	-	-	-	ν_{NH}
-	-	3126	-	-	$\nu_{\equiv CH}$
3006	-	-	-	-	ν_{CH} a.s.
2965	-	-	-	-	ν_{CH}
2922	-	-	-	-	ν_{CH} s.
-	-	2083/2052	2083/2052	-	$\nu_{C\equiv^{14}N}$ / $\nu_{C\equiv^{15}N}$
1704	-	-	-	-	$\nu_{C=O}$
-	1635	1635	-	-	δ_{NH} and overtone of $\delta_{\equiv CH}$
-	-	-	-	1480	δ_{NH}
1422	-	-	-	-	δ_{CH}
1369	-	-	-	-	δ_{CH}
1357	-	-	-	-	δ_{CH}
1237	-	-	-	-	$\nu_{C\text{-}C}$ a.s.
-	1109	-	-	-	ω_{NH}
1096	-	-	-	-	ρ_{CH}
900	-	-	-	-	ρ_{CH}
-	-	824	-	-	$\delta_{\equiv CH}$

s: symmetric; a.s.: antisymmetric; i.p: in plane. ν: stretching δ: bending ρ: rocking ω: wagging

These attributions point out the possible formation of 2-hydroxy-2-methylpropanenitrile (HO-$C(CH_3)_2$-CN), which would come from the reaction between acetone and CN^-. The residues are further analysed by monitoring their mass spectrum during their desorption at 197 K (Figure 2C). The *m/z* 85 peak (corresponding to HO-$C(CH_3)_2$-CN) is not directly observed as the 70 eV impact electronic source of the mass spectrometer is exceedingly energetic and breaks HO-$C(CH_3)_2$-CN into smaller fragments. The *m/z* 70 fragment can be assigned to the loss of a methyl group. This fragment shifts to *m/z* 71 in the experiment using ^{15}N, strengthening the

hypothesis of the presence of HO-C(CH_3)$_2$-CN. Other fragments at *m/z* 58 and *m/z* 43 can respectively be attributed to the loss of HCN and the loss of HCN+CH_3. These fragments do not shift when ^{15}N is used, because the C≡N moiety is already lost.

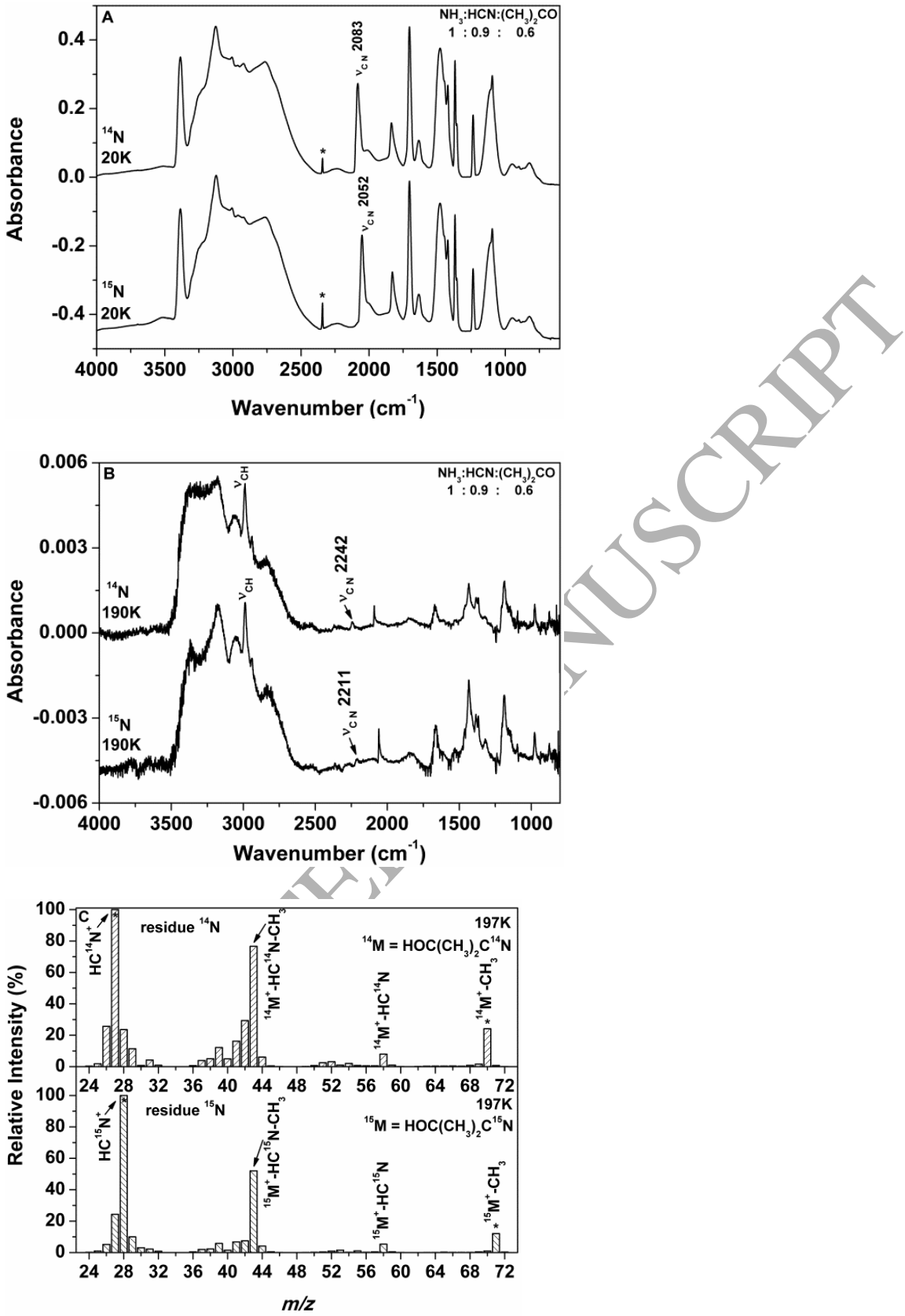

Figure 2: (A) Infrared spectra of NH_3:HCN:$(CH_3)_2CO$ 1:0.9:0.6 ices deposited at 20 K with $HC^{14}N$ (upper spectrum) or $HC^{15}N$ (bottom spectrum). The band marked with * corresponds to CO_2 contamination. (B) Infrared spectra of the residues of the same ices after being warmed at 4 K min^{-1} to 190 K. Characteristic bands

are displayed on each spectrum. (C) Mass spectra (electron impact ionization 70 eV) of the residues of the same ices at their maximum of desorption (197 K). Various fragments are identified, and the shifts due to ^{15}N are noted with *.

Table 2: Infrared band positions of the residues from NH_3:HCN:$(CH_3)_2CO$ 1:0.9:0.6; $(CH_3)_2CO$:H_2O:$^{14}NH_3$:$HC^{15}N$ 1:1:0.6:0.3; and $(CH_3)_2CO$:H_2O:$^{15}NH_3$:$HC^{14}N$ 1:1:0.6:0.3 ices heated at 4 K min^{-1} to 190 K, and their attributions, compared to $HOC(CH_3)_2CN$ standard at 20 K and to B3LYP-D2* calculated values.

Band positions (cm^{-1})					
$(CH_3)_2CO$: $HC^{14}N$:NH_3 1:0.9:0.6	$HOC(CH_3)_2CN$ standard	B3LYP-D2*	$(CH_3)_2CO$:H_2O: $^{14}NH_3$:$HC^{15}N$ 1:1:0.6:0.3	$(CH_3)_2CO$:H_2O: $^{15}NH_3$:$HC^{14}N$ 1:1:0.6:0.3	Attributions
3375	3402	3550 - 3250	-	-	ν_{OH}
3175	-	-	3169	3169	ν_{NH} + δ_{NH} of NH_4^+
3053	-	-	3031	3031	ν_{NH} of NH_4^+
2988	2993	3031	2988	2988	ν_{CH} a.s.
2940	2944	2942	-	-	ν_{CH} s.
2832	-	-	2836	2825	$2\delta_{NH}$ of NH_4^+
2243/2211	2248	2290	2209	2241	$\nu_{C\equiv{}^{14}N}$ / $\nu_{C\equiv{}^{15}N}$
2091/2059	-	-	2060	2091	$\nu_{C\equiv N}$ of CN^-
-	2086	-	-	-	$\nu_{C\equiv N}$ of HCN
-	1700	-	-	-	$\nu_{C=O}$ of acetone
1667	-	-	1674	1674	δ_{OH}
-	1466	1467	-	-	δ_{CH3} a.s. [a]
1434	-	-	1436	1432	δ_{NH} of NH_4^+
-	1420	1418 [b]	-	-	δ_{OH} i.p. + δ_{CH3} s. [a]
1385	1383	1385	1386	1386	δ_{OH} i.p. + δ_{CH3} s. [a]
1368	1368	1357	1368	1367	δ_{OH} i.p. + δ_{CH3} s. [a]
1188	1192	1163	1193	1193	δ_{OH} i.p. [a]
1151	1154	1141	1148	1150	δ_{OH} i.p. [a]
1097	1096	1121 [b]	1097	1097	δ_{OH} i.p. [a]
976	978	959	978	978	$\nu_{C\text{-}OH}$ [a]
874	876	860	-	-	$\nu_{C\text{-}C\equiv N}$ [a]

[a] Attributions from visual inspection of the calculated vibrational frequencies. [b] Overlapped bands. s: symmetric; a.s.: antisymmetric; i.p: in plane. ν: stretching δ: bending ρ: rocking ω: wagging

In order to confirm the HO-$C(CH_3)_2$-CN formation, our residue was compared to a 2-hydroxy-2-methylpropanenitrile standard deposited and heated in the same conditions (Figure 3A). HCN ($\nu_{C\equiv N}$ at 2083 cm^{-1}) and acetone ($\nu_{C=O}$ at 1704 cm^{-1}) are visible in the IR spectrum of the standard. This is probably because 2-hydroxy-2-methylpropanenitrile can be dissociated into acetone and HCN in the gas phase before being deposited on the sample holder, leading to their presence in the ice. Bands were attributed with the help of a theoretical IR spectrum (Figure 3A). Table 2 summarizes all band attributions. Most of the bands of the residue perfectly match with those of the standard. Namely, ν_{CH} a.s. and s. at 2988 cm^{-1} and 2940 cm^{-1}, $\nu_{C\equiv N}$ at 2243 cm^{-1}, δ_{OH} at 1188 cm^{-1} and 1097 cm^{-1}, $\nu_{C\text{-}OH}$ at 976 cm^{-1} and $\nu_{C\text{-}C\equiv N}$ at 874 cm^{-1} strongly support the hypothesis of the formation of a HO-$C(CH_3)_2$-CN residue, especially since the relative intensities of the bands are similar.

Interestingly, the IR spectrum of the standard 2-hydroxy-2-methylpropanenitrile is shown at 20 K, because it crystallizes when heated at 190 K, making the infrared bands thinner and higher, hampering a suitable comparison. In contrast, no crystallization is observed in our residue, which might be due to the very low amount of 2-hydroxy-2-methylpropanenitrile produced in the residue, making it impossible to structure itself into crystals. Furthermore, bands at 1434 cm^{-1} (δ_{NH}) and 2091 cm^{-1} ($\nu_{C\equiv N}$) show that the [NH_4^+ $^-$CN] salt is still present at 190 K, and probably influences the structure of 2-hydroxy-2-methylpropanenitrile.

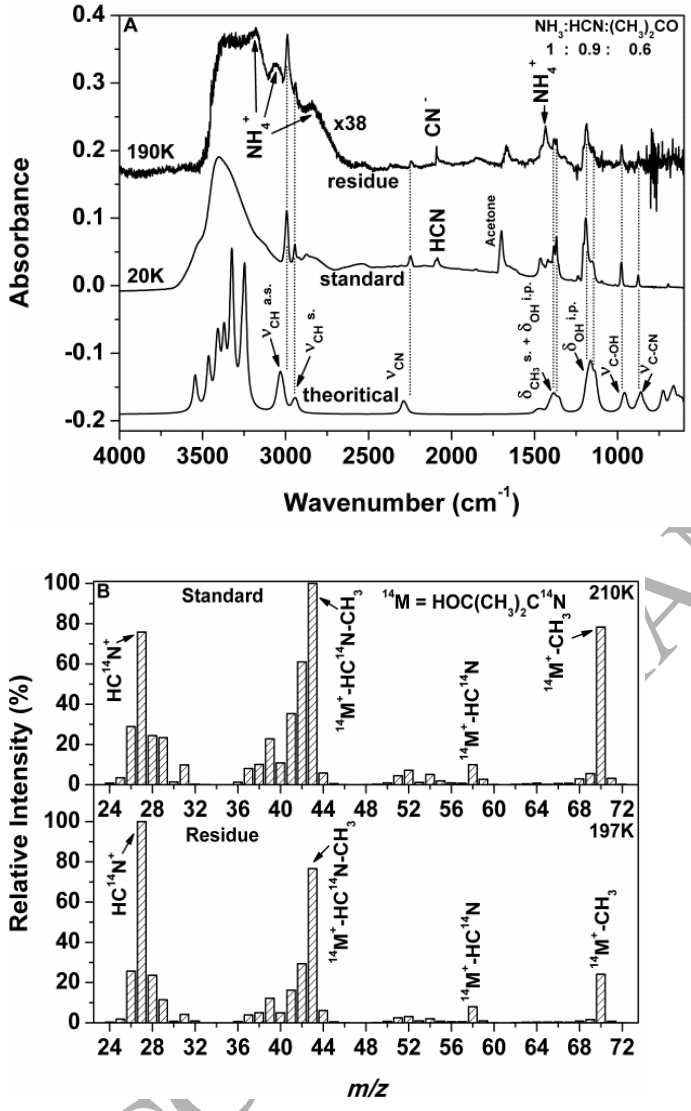

Figure 3: (A) Infrared spectra of the residue of a NH_3:$HC^{14}N$:$(CH_3)_2CO$ 1:0.9:0.6 ice deposited at 20 K and warmed at 4 K min^{-1} to 190 K, and of 2-hydroxy-2-methylpropanenitrile ($HOC(CH_3)_2CN$) standard deposited at 20 K. These spectra are compared to the theoretical spectrum of $HOC(CH_3)_2CN$. (B) Mass spectra of 2-hydroxy-2-methylpropanenitrile ($HOC(CH_3)_2CN$) standard at 210 K (upper panel), and of the residue of a NH_3:$HC^{14}N$:$(CH_3)_2CO$ 1:0.9:0.6 ice at 197 K (bottom panel).

The mass spectra of the standard 2-hydroxy-2-methylpropanenitrile and the residue are compared in Figure 3B. The same fragments are detected with similar relative intensities. The *m/z* 85 peak is also not directly detected in the standard, confirming that the ionization process breaks the molecule into fragments. Comparison with the mass spectrum of 2-hydroxy-2-methylpropanenitrile found in the National Institute of Standards and Technology

(NIST) Chemistry WebBook is also consistent. HO-C$(CH_3)_2$-CN is thus formed in the solid phase by heating a NH_3:HCN:$(CH_3)_2$CO ice.

It is worth mentioning that the reaction does not proceed with only HCN and acetone in the ice (i.e. in the absence of NH_3) because HCN needs to be activated into CN^- in order to react with acetone. The nucleophilic attack of NH_3 activates HCN, allowing the formation of HO-C$(CH_3)_2$-CN. The same results have already been found when acetone is replaced by formaldehyde (CH_2O) (Danger et al., 2012) or acetaldehyde (CH_3CHO) (Fresneau et al., 2015). Contrarily to what happens with aldehydes, the aminoalcohol is not formed from a NH_3:HCN:$(CH_3)_2$CO ice. This is expected because NH_3 and $(CH_3)_2$CO must be trapped in the water matrix long enough to allow them to form 2-aminopropan-2-ol during the warming (Fresneau et al., 2014).

3.2 H_2O:HCN:$(CH_3)_2$CO and H_2O:NH_3:HCN:$(CH_3)_2$CO ice reactivity

With formaldehyde and acetaldehyde, it has been shown that the reaction leading to the corresponding hydroxynitrile can still occur with H_2O instead of NH_3. Indeed, H_2O is thought to be able to activate HCN into CN^-. Here we test this with a H_2O:HCN:$(CH_3)_2$CO 1:0.6:0.2 ice mixture (Figure 4). Unexpectedly, no reaction is observed upon warming the ice; only the desorption of the reactants occurs. Water desorbs at 180 K, and the IR spectrum at 185 K is back to the baseline. This indicates differences in the activation of HCN when reacting with formaldehyde or acetaldehyde. We discuss possibilities of the different roles of H_2O in these reactions in section 4.

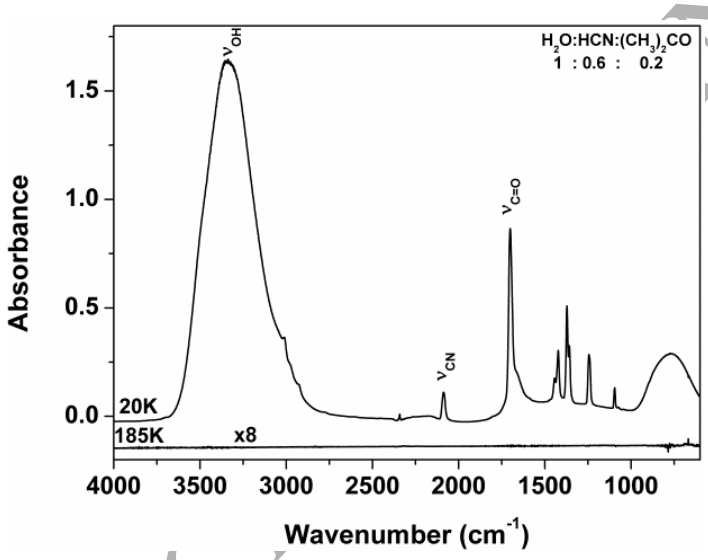

Figure 4: Infrared spectrum of a H_2O:HCN:$(CH_3)_2$CO 1:0.6:0.2 ice deposited at 20 K and warmed to 185 K.

We also know that acetone can react with ammonia to form 2-aminopropan-2-ol (H_2N-C$(CH_3)_2$-OH), but only in the presence of water (Fresneau et al., 2014), because water traps ammonia and acetone in the solid phase above their desorption temperature, thereby allowing the reaction to occur. The activation energy of 2-hydroxy-2-methylpropanenitrile is probably lower than that of 2-aminopropan-2-ol, since we showed in section 3.1 that the former does not need H_2O to trap the reactants in the solid phase for the reaction to occur. Therefore, even if water is added to a NH_3:HCN:$(CH_3)_2$CO ice, acetone will most likely be consumed to form 2-hydroxy-2-methylpropanenitrile over 2-aminopropan-2-ol.

In order to test the potential competition between 2-hydroxy-2-methylpropanenitrile and 2-aminopropan-2-ol formation, different $(CH_3)_2$CO:H_2O:NH_3:HCN ices are studied. The $(CH_3)_2$CO:NH_3:H_2O ratios are chosen to

match ratios used in Fresneau *et al.* (Fresneau et al., 2014) that are known to lead to the formation of 2-aminopropan-2-ol, and HCN is added to the mixture. Experiments with $^{15}NH_3$ and $HC^{15}N$ are conducted to help product identification. The two ices studied are a $(CH_3)_2CO:H_2O:^{14}NH_3:HC^{15}N$ 1:1:0.6:0.3 ice and a $(CH_3)_2CO:H_2O:^{15}NH_3:HC^{14}N$ 1:2:0.6:0.6 ice. IR spectra of the residues of these ices at 190 K are displayed in Figure 5. The comparison with a 2-hydroxy-2-methylpropanenitrile standard seems to indicate its presence in the residues, similarly to the case of an NH_3:HCN:$(CH_3)_2CO$ ice (Figure 3A). The shift of $\nu_{C\equiv N}$ from 2241 to 2209 cm^{-1}, ν_{CH} a.s. at 2988 cm^{-1}, δ_{OH} at 1193 cm^{-1}, and $\nu_{C\text{-}OH}$ at 978 cm^{-1} all tend to show that 2-hydroxy-2-methylpropanenitrile was formed, whereas no characteristic feature of 2-aminopropan-2-ol is visible. Band attributions are summarized in Table 2.

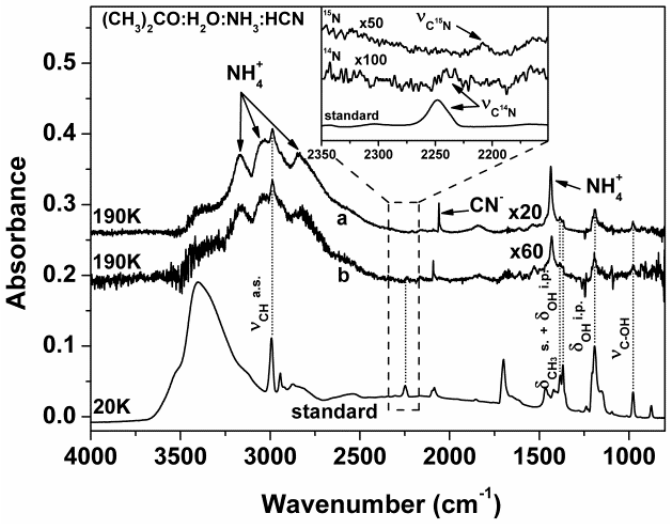

Figure 5: Infrared spectra of the residue of: (a) a $(CH_3)_2CO:H_2O:^{14}NH_3:HC^{15}N$ 1:1:0.6:0.3 ice; (b) a $(CH_3)_2CO:H_2O:^{15}NH_3:HC^{14}N$ 1:2:0.6:0.6 ice; both deposited at 20 K and warmed at 4 K min^{-1} to 190 K. These are compared to a 2-hydroxy-2-methylpropanenitrile ($HOC(CH_3)_2CN$) standard deposited at 20 K.

These results are supported by the comparison of the temperature programmed desorption (TPD) of the same $(CH_3)_2CO:H_2O:^{14}NH_3:HC^{15}N$ 1:1:0.6:0.3 (Figure 6A) and $(CH_3)_2CO:H_2O:^{15}NH_3:HC^{14}N$ 1:2:0.6:0.6 ices (Figure 6B) with the TPD of a $(CH_3)_2CO:H_2O:^{14}NH_3$ 1:0.6:0.4 ice (Figure 6C) reproduced from Fresneau et al. (Fresneau et al., 2014) as a reference for 2-aminopropan-2-ol.

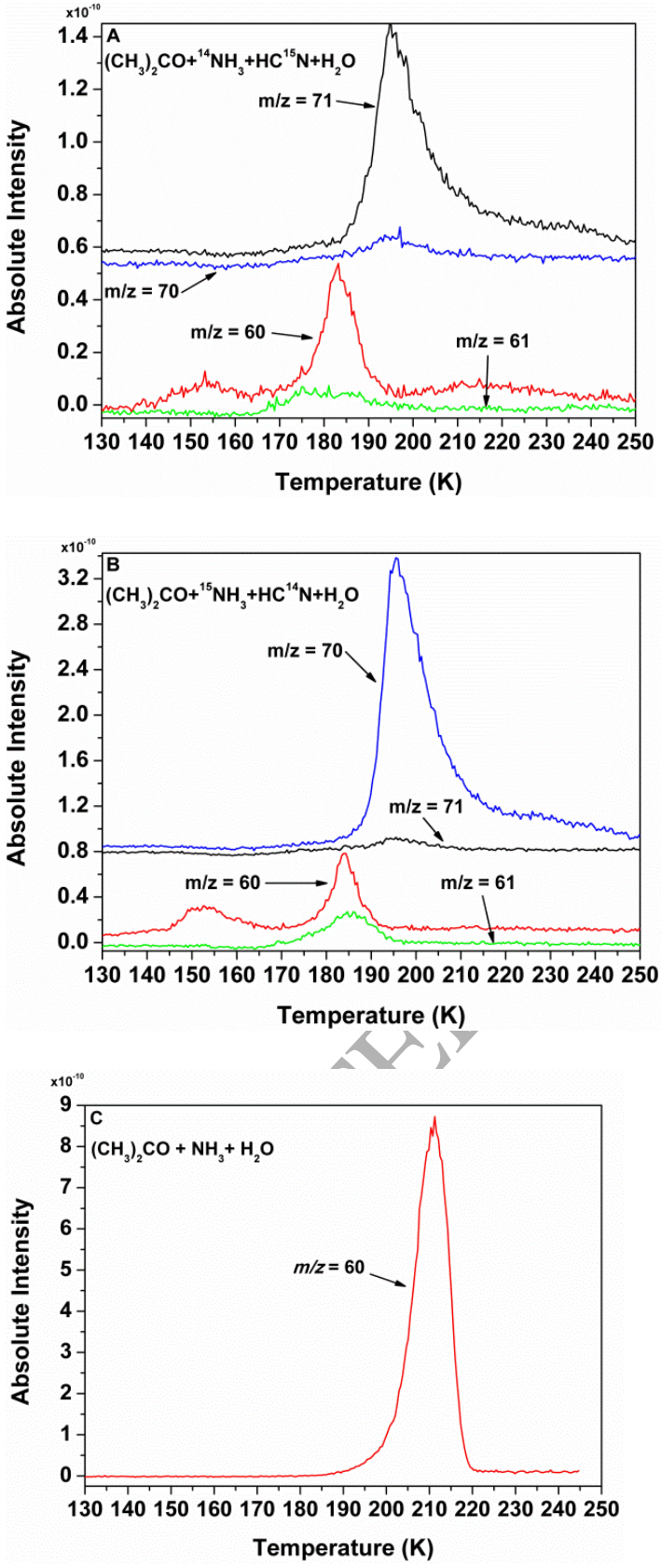

Figure 6: Temperature programmed desorption (TPD) obtained by monitoring *m/z* 60, 61, 70 and 71 of ices containing (A) $(CH_3)_2CO$:H_2O:$^{14}NH_3$:$HC^{15}N$ 1:1:0.6:0.3, (B) $(CH_3)_2CO$:H_2O:$^{15}NH_3$:$HC^{14}N$ 1:2:0.6:0.6 and (C)

$(CH_3)_2CO:H_2O:^{14}NH_3$ 1:0.6:0.4 (reproduced from Fresneau *et al.* (Fresneau et al., 2014)) . Temperature ramp 4K min^{-1}.

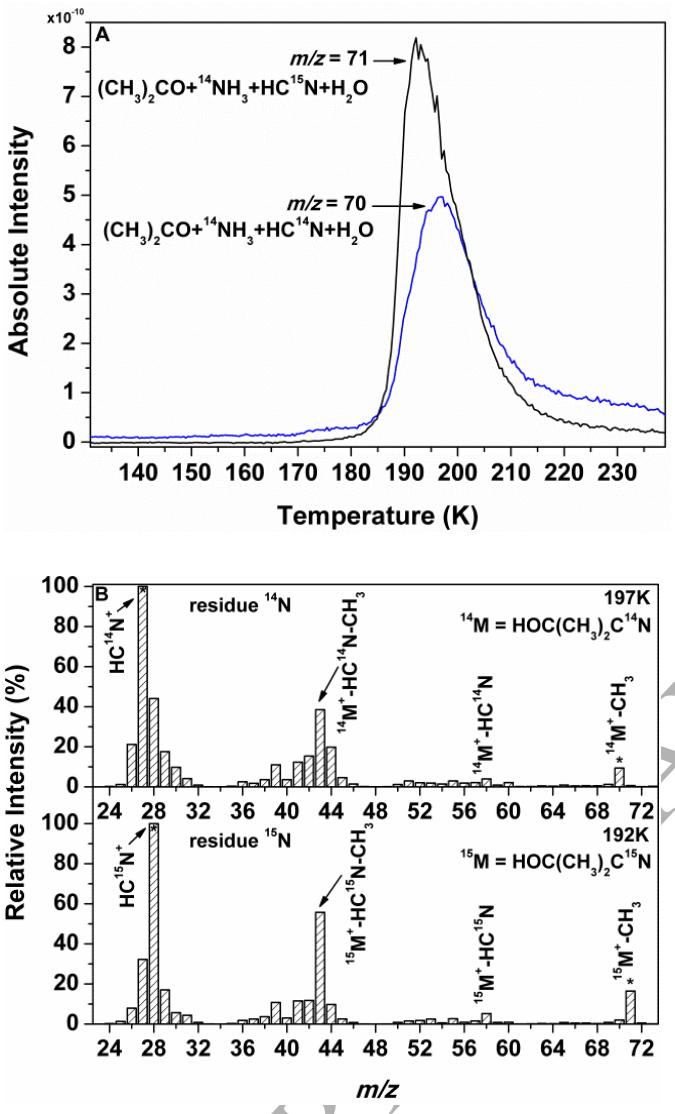

Figure 7: (A) Temperature programmed desorption (TPD) of $H_2O:NH_3:HCN:(CH_3)_2CO$ 1:0.2:0.2:0.1 ices deposited at 20 K with $HC^{14}N$ or $HC^{15}N$ obtained by monitoring respectively the fragment *m/z* 70 and the fragment *m/z* 71. (B) Mass spectra (electron impact ionization 70 eV) of the residues of the ices described in Figure 7A at their maximum of desorption. Various fragments are identified, and the fragments shifting in the presence of $H^{15}CN$ are noted with *.

All the observed fragments correspond to the loss of a CH_3 group. Peaks at *m/z* 60, 61, 70 and 71 correspond to fragments coming from $_2H^{14}N$-$C(CH_3)_2$-OH, $_2H^{15}N$-$C(CH_3)_2$-OH, HO-$C(CH_3)_2$-$C^{14}N$ and HO-$C(CH_3)_2$-$C^{15}N$, respectively. The formation of 2-hydroxy-2-methylpropanenitrile in both ices containing HCN is confirmed by the *m/z* 70 peak at ~195 K (Figure 6B), which shifts to *m/z* 71 (Figure 6A) in the $HC^{15}N$ experiment. On the other hand, the presence of 2-aminopropan-2-ol is not so clear. If 2-aminopropan-2-ol had been formed in the ices containing HCN in similar amounts to the $(CH_3)_2CO:NH_3:H_2O$ ice (Figure 6C), a shift of the *m/z* 60 peak to *m/z* 61 in the experiment using $^{15}NH_3$ should have been observed at ~210 K. However, this is not the case in

Figure 6 (A & B). Instead, a *m/z* 60 peak is observed at 185 K in both experiments using $^{14}NH_3$ and $^{15}NH_3$, during water desorption. It has been shown (Fresneau et al., 2014) that when 2-aminopropan-2-ol is formed at a very low yield, it co-desorbs with water at 185 K. If it was the case here, the *m/z* 60 peak at 185 K in the $^{14}NH_3$ experiment (Figure 6A) should shift to *m/z* 61 in the $^{15}NH_3$ experiment (Figure 6B). A small increase of the *m/z* 61 peak is indeed observed on the experiment using $^{15}NH_3$, which could indicate the presence of 2-aminopropan-2-ol in trace amounts. However, the m/z 60 peak does not show a noticeable difference between the $^{14}NH_3$ and the $^{15}NH_3$ experiment, meaning that another unidentified molecule co-desorbs with water. It is seen in the acetone reference spectrum (acetone or acetone + H_2O), which suggests that the m/z 60 peak might be an impurity present in acetone. Even if traces amount of 2-aminopropan-2-ol may have been formed in both experiments containing HCN, this is far from what is obtained with similar ratios in the absence of HCN (Figure 6C). This proves that the formation of 2-hydroxy-2-methylpropanenitrile is favored over the formation of 2-aminopropan-2-ol.

For a more astrophysical relevant approach, we deposit H_2O:NH_3:HCN:$(CH_3)_2CO$ 1:0.2:0.2:0.1 ices at 20 K containing either $HC^{14}N$ or $HC^{15}N$. By monitoring *m/z* 70 ($HC^{14}N$) and *m/z* 71 ($HC^{15}N$) during the warming (Figure 7A), 2-hydroxy-2-methylpropanenitrile is observed and desorbs around 195 K. This is confirmed by the mass spectra displayed at the maximum of desorption for each residue (Figure 7B) which are very similar to the 2-hydroxy-2-methylpropanenitrile standard shown in Figure 3B. As expected from the results displayed in Figure 6, no clear evidence of 2-aminopropan-2-ol formation has been found with these ratios. If 2-aminopropan-2-ol has been formed, it is below the detection limits of mass spectrometry, i.e. in trace amount.

3.3 calculation of the activation energy of 2-hydroxy-2-methylpropanenitrile

Sections 3.1 and 3.2 show that 2-hydroxy-2-methylpropanenitrile is formed in the solid phase when ices containing NH_3, HCN and $(CH_3)_2CO$, in the presence or not of H_2O, are warmed. The activation energy of the 2-hydroxy-2-methylpropanenitrile formation cannot be deduced from the IR spectra of the experiment. We do witness the appearance of the $\nu_{C\equiv N}$ band at 2243 cm^{-1} between 140 K and 150 K, meaning that the reaction starts to occur between those temperatures, but the uncertainty on the measure of the area of this band during its growth is too high to calculate the activation energy reliably. Because of this experimental limitation, we use quantum chemical simulations to calculate the energy barriers for the formation of this molecule.

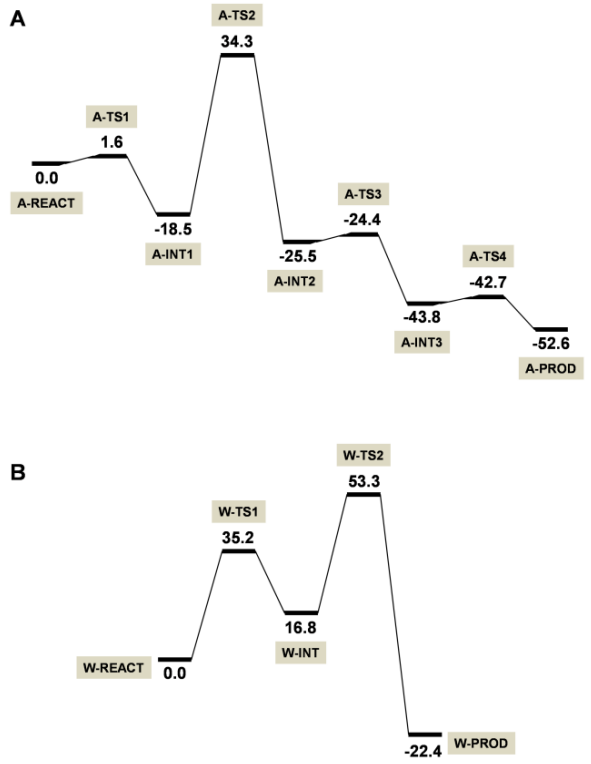

Figure 8: Potential energy profiles (in kJ mol^{-1}), with respect to A-REACT, for the formation of $HOC(CH_3)_2CN$ from reaction between HCN and acetone in a H_2O-dominated ice model (A) in the presence of NH_3 and (B) in the absence of NH_3.

We characterize the potential energy surface (PES) of the mechanistic steps involved in the reaction. Figure 8A shows the calculated PES and Figure 9 the optimized stationary points involved. These calculations are based on a cluster approach; that is, the ice mixture is modelled by a finite cluster consisting of 31 H_2O molecules, one NH_3, one HCN and one acetone molecule (see A-REACT). This A-REACT initial state has the NH_3, HCN and acetone molecules engaged by hydrogen bonds (H-bonds) on the H_2O-dominated cluster, with the particularity that NH_3 and HCN are interacting through a strong H-bond. The reaction involves four steps: step i) a proton transfer from HCN to NH_3 (A-TS1), in which the NH_4^+/CN^- ion pair is formed (A-INT1); step ii) a C-C coupling between the CN^- and acetone (A-TS2), which leads to the formation of the deprotonated form of 2-hydroxy-2-methylpropanenitrile ($^-OC(CH_3)_2CN$, A-INT2); and steps iii) and iv) protonation of $^-OC(CH_3)_2CN$ from the NH_4^+ ion and through a proton relay mechanism assisted by water molecules (A-TS3, A-INT3 and A-TS4) to form the final product (A-PROD). Table 3 summarizes the calculated relative (with respect to A-REACT) potential energies including zero-point energy corrections (ΔU^0_{rel}) and the relative free energies (ΔG_{rel}) at 20 K and 190 K, which are the initial and final temperatures of the experiments. Note that the energy profiles shown in Figure 8 are built from the relative potential energy values whereas Table 3 data report ΔU^0_{rel} and ΔG_{rel} values and accordingly they are different. Table 4 reports the intrinsic energy barriers ($\Delta G^{\neq}$) of each step, the rate constants (k) calculated using the classical Eyring equation and the corresponding half-life times (time necessary to consume half the amount of reactant, $t_{1/2}$) to assess their speed. The calculated reaction energies are negative and accordingly formation of 2-hydroxy-2-methylpropanenitrile is favorable.

Table 3: Relative energy values (in kJ mol^{-1}) of the stationary points involved in Figure 8 (A & B): ΔU^0_{rel}, relative potential energy values including zero-point energy corrections; and ΔG_{rel}, relative free energies at 20 and 190 K.

Stationary point	ΔU^0_{rel}	ΔG_{rel} (T = 20 K)	ΔG_{rel} (T = 190 K)
A-REACT	0.0	0.0	0.0
A-TS1	-5.2	-5.1	-3.8
A-INT1	-10.7	-10.6	-5.8
A-TS2	40.2	40.3	50.5
A-INT2	-14.4	-14.2	0.7
A-TS3	-18.4	-18.1	-2.3
A-INT3	-26.8	-26.6	-11.2
A-TS4	-30.7	-30.5	-14.2
A-PROD	-34.4	-34.2	-21.8
W-REACT	0.0	0.0	0.0
W-TS1	23.7	23.8	29.7
W-INT	13.7	13.8	17.2
W-TS2	52.1	52.1	59.7
W-PROD	-10.4	-10.3	-3.9

Concerning the energy barriers, data from Table 3 indicates that, upon inclusion of zero-point energy (ZPE) corrections and entropic effects, the proton transfer from HCN to NH_3 is barrierless (i.e., A-TS1 is lower in energy than A-REACT) and accordingly, the NH_4^+/CN^- ion pair is spontaneously formed when the NH_3 and HCN ices are in contact. This is in perfect agreement with the experimental findings, in which bands associated to the formation of this salt are identified after deposition. Among the other subsequent steps, the reaction between CN^- and acetone (step ii) is the only one presenting a sizeable energy barrier. For the other two (steps iii and iv), when ZPE and entropic corrections are considered, the corresponding transition states are more stable than the corresponding previous intermediates (see Table 3). Accordingly, step ii is the rate determining step with $\Delta G^{\neq}$ = 50.9 and 56.4 kJ mol^{-1} at 20 and 190 K, respectively. The calculated k and $t_{1/2}$ values indicate that at 20 K this step does not proceed because it is kinetically hindered, whereas at 190 K the reaction can favorably evolve with $t_{1/2} \approx$ 9 minutes.

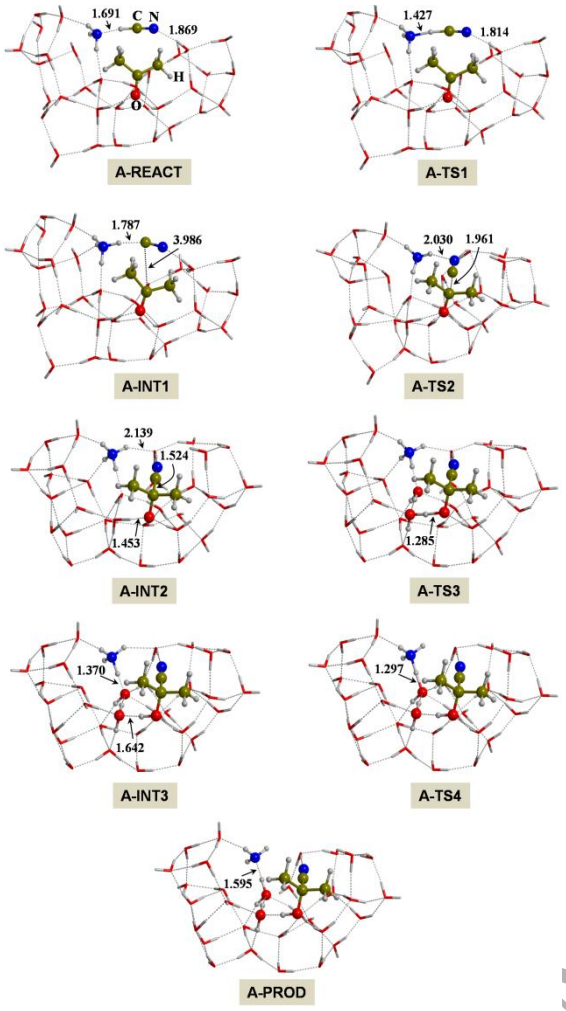

Figure 9: B3LYP-D3/6-31+G(d,p)-optimized geometries of the stationary points involved in the formation of $HOC(CH_3)_2CN$ from reaction between HCN and acetone in a H_2O-dominated ice model in the presence of NH_3 (namely, the PES represented in Figure 8A).

Table 4: Intrinsic free energy barriers ($\Delta G^{\neq}$, in kJ mol^{-1}) of the steps involved in Figure 8 (A & B), calculated rate constants (k, in s^{-1}), and half-life times ($t_{1/2}$, in s) at 20 and 190 K.

	A-INT1 → A-TS2	W-REACT → W-TS1	W-INT1 → W-TS2
20 K			
$\Delta G^{\neq}$	50.9	23.8	52.1
k	4.2×10^{-122}	3.5×10^{-51}	2.7×10^{-125}
$t_{1/2}$	1.6×10^{121}	1.9×10^{50}	2.6×10^{124}
190 K			
$\Delta G^{\neq}$	56.4	29.7	59.7
k	1.3×10^{-3}	2.7×10^{4}	1.5×10^{-4}
$t_{1/2}$	5.5×10^{2}	2.6×10^{-5}	4.6×10^{3}

We also use these quantum chemical methods to simulate the same reaction in the absence of NH_3. Figure 8B presents the calculated PES of this process and Figure 10 shows the optimized structures. For the sake of consistency with the calculated reaction with NH_3, a similar finite cluster model has been used in which the NH_3 molecule is replaced by one H_2O (see W-REACT of Figure 10). At variance with NH_3, this reaction presents

only two steps: step i) a proton transfer from HCN to a H_2O molecule belonging to the ice (W-TS1), which takes place through a proton relay mechanism and leads to the formation of a H_3O^+/CN^- ion pair (in this case the H_3O^+ and CN^- ions are separated by several water molecules, see W-INT); and step ii) coupling between CN^- and acetone (W-TS2), which is spontaneously followed by the proton transfer from the H_3O^+ to the organic moiety to form the final $HOC(CH_3)_2CN$ (W-PROD). Calculated values presented in Table 3 indicate that the first step has a sizeable energy barrier that cannot be overcome at 20 K ($\Delta G^{\neq}$ = 23.8 kJ mol^{-1} and $t_{1/2} \approx 10^{50}$ s). This agrees with the experimental findings because, upon ice deposition, features associated with the formation of a $[H_3O^+CN^-]$ salt are not observed, contrarily to with NH_3, in which the $NH_4^+CN^-$ salt forms. Despite this, the first step is surmountable at 190 K ($t_{1/2} \approx 10^{-5}$ s). At this temperature, the second step, presenting the highest energy barrier values, was computed to have $\Delta G^{\neq}$ = 59.7 kJ mol^{-1}, which means a $t_{1/2} \approx 77$ minutes. This estimated $t_{1/2}$ is long considering that the warming of the ices to form the products takes about 45 minutes (from 20 to 190 K with a temperature ramp of 4 K min^{-1}). These results suggest that $HOC(CH_3)_2CN$ can form but in low amounts. These results are in line with the experiments because formation of hydroxy-2-methylpropanenitrile from a H_2O:HCN:$(CH_3)_2CO$ ice mixture is not observed (see section 3.2).

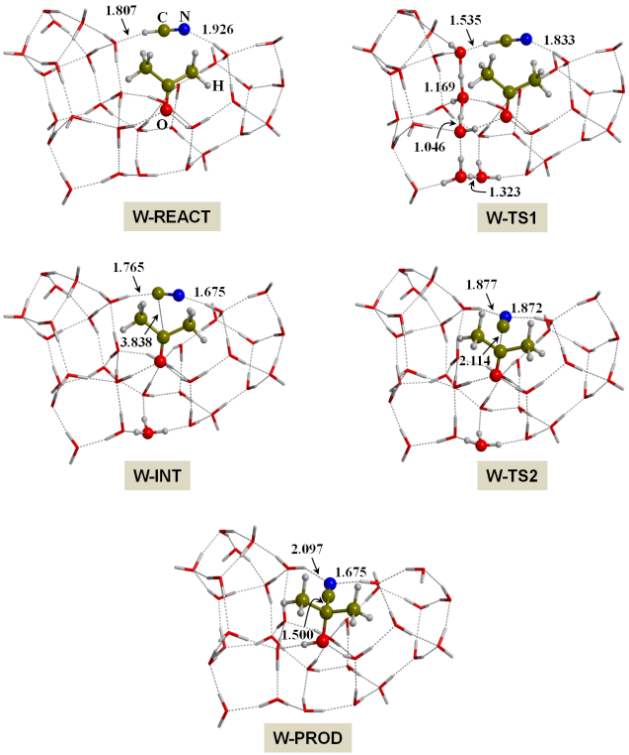

Figure 10: B3LYP-D3/6-31+G(d,p)-optimized geometries of the stationary points involved in the formation of $HOC(CH_3)_2CN$ from reaction between HCN and acetone in a H_2O-dominated ice model in the absence of NH_3 (namely, the PES represented in Figure 8B).

4 Discussion

According to the results described in section 3, no reaction seems to occur during the warming of ices containing H_2O, HCN and $(CH_3)_2CO$. The formation of 2-hydroxy-2-methylpropanenitrile ($HOC(CH_3)_2CN$) was expected since previous works on H_2O:HCN:CH_2O (formaldehyde) and H_2O:HCN:CH_3CHO (acetaldehyde) ices led to the formation of hydroxyacetonitrile ($HOCH_2CN$) (Danger et al., 2012) and 2-hydroxypropionitrile

(HOCH(CH_3)CN) (Fresneau et al., 2015), respectively. None of these reactions take place when only HCN and an aldehyde are mixed (i.e., absence of H_2O). Thus, formation of a hydroxynitrile is activated in the presence of water, thanks to a mechanism similar to that simulated in Figure 9; that is, the interaction between H_2O and HCN leads to the formation of H_3O^+ and CN^-, and CN^- reacts with the aldehyde to form the hydroxynitrile. Beside the differences in the methods and the cluster models used to simulate the formation of hydroxynitriles through reaction of HCN with H_2CO, CH_3CHO, or $(CH_3)_2CO$, quantum chemical results indicate that: i) the calculated potential energy barriers of the rate determine step (in all cases, the NC-CO coupling) are about 50 – 55 kJ mol^{-1}; and ii) formation of the H_3O^+/CN^- ion pair is an unfavorable process as the ion pair intermediates are higher in energy than the reactant structures, meaning that, in practice, the reaction can be considered as concerted in which the formation of the H_3O^+/CN^- is immediately followed by the NC-CO coupling. Because of these similarities between the reactions involving H_2CO, CH_3CHO and $(CH_3)_2CO$, a reasonable explanation why the reaction does not work in a H_2O:HCN:$(CH_3)_2CO$ ice can come from the fact that the diffusion of acetone to encounter the CN^- ion is slower than formaldehyde and acetaldehyde due to the larger size of the former. Moreover, the larger steric hindrance of acetone due to the presence of two CH_3 groups, which can hamper the attack of the CN^- on the CO, can also play a role. This minor chemical activity of acetone has actually been observed when reacting with NH_3. The measured overall activation energies of the reaction of NH_3 with formaldehyde, acetaldehyde and acetone are ≈ 4.5 kJ mol^{-1} (Bossa, Theulé, et al., 2009), 33 kJ mol^{-1} (Duvernay et al., 2010) and 42 kJ mol^{-1} (Fresneau et al., 2014), which is probably due to the lower diffusion and larger steric hindrances of the bigger compounds. In contrast, our results show that an NH_3:HCN:$(CH_3)_2CO$ ice leads to the formation of 2-hydroxy-2-methylpropanenitrile. In this case, the [NH_4^+ $^-$CN] salt is formed in the ice (Noble et al., 2013), which is clearly identified with the bending mode δ_{NH} of NH_4^+ at 1480 cm^{-1} (Figure 2A & Table 1) and supported by the favorable energetic data associated with the formation of the NH_4^+/CN^- ion pair. This means that the actual reactant is the salt, and accordingly, the HCN is activated in the form of CN^- ion, which in turn is ready to react with acetone, and hence, probably, the formation of the product.

The reactions described in this work are related to the occurrence of the Strecker synthesis on or in ices of interstellar and cometary grains when they are warmed. The Strecker synthesis requires H_2O, NH_3, HCN, and aldehydes/ketones. The present work focuses on the study of acetone, the smallest ketone. Studying the thermal evolution of H_2O:NH_3:HCN:$(CH_3)_2CO$ ices is of interest for astrochemistry, as it can help assessing the possibilities to form amino acid precursors in astrophysical environments. The four components of this ice have all indeed been detected in dense molecular clouds via radioastronomy. Acetone has been detected in the ISM, in both Sagittarius B2 (Combes et al., 1987; Snyder et al., 2002) and the Orion-KL star forming region (Friedel et al., 2005). It has also been found in the Murchison meteorite. HCN (Snyder and Buhl, 1971; Boonman et al., 2001) and NH_3 (Cheung et al., 1968) have been detected in the ISM as well, but also in the comae of comets (Bockelée-Morvan et al., 2004). Even though these molecules have been detected in the gas phase and not yet in the infrared spectra of interstellar ices, it does make sense to suppose that HCN, NH_3 and $(CH_3)_2CO$ can be found on the icy mantles of interstellar grains, where they can react when the grain is being thermally processed during the formation of a protostar.

If we wanted to simulate more accurately an astrophysical ice, we would have to consider ratios such as H_2O:NH_3:HCN:$(CH_3)_2CO$ 4000:40:10:1 (Lara et al., 2004) or 4000:28:10:1 (Crovisier and Bockelée-Morvan, 1999), which would be below the detection limits of our experimental system. Even though the real abundances

of those four compounds in our experiment do not reflect their respective ratio in natural environments, abundance orders between the species are respected. This gives an idea of the possible chemical pathways and what molecules could be formed on grains. From H_2O:NH_3:$(CH_3)_2CO$ ices it has been shown that 2-aminopropan-2-ol ($H_2NC(CH_3)_2OH$) is formed (Fresneau et al., 2014), which is the first step of the Strecker reaction that would lead to aminoisobutionitrile ($NH_2C(CH_3)_2CN$), a precursor to 2-aminoisobutyric acid ($NH_2C(CH_3)_2COOH$). Here, we showed that when HCN is added to a H_2O:NH_3:$(CH_3)_2CO$ mixture, acetone is consumed to form exclusively 2-hydroxy-2-methylpropanenitrile ($HOC(CH_3)_2CN$) because this reaction is favored over the formation of 2-aminopropan-2-ol. This implies that it is unlikely to go any further than 2-aminopropan-2-ol in the Strecker synthesis with acetone. This reaction pathway towards the formation of aminoisobutionitrile appears to be impossible in the solid phase. This is not the case for formaldehyde and acetaldehyde.

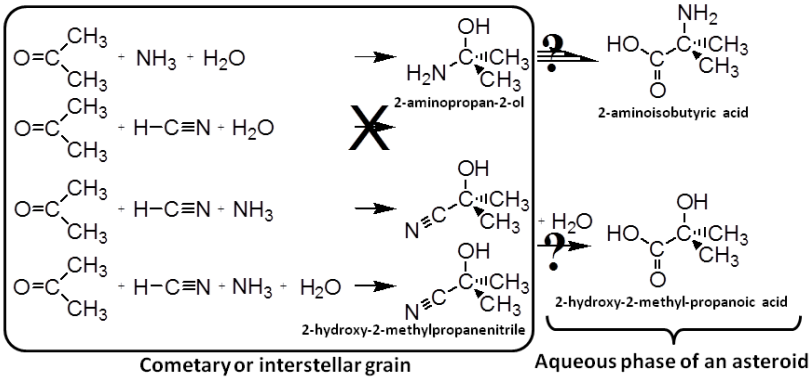

Figure 11: Summary of the thermal reactivity of ices containing acetone, ammonia, hydrogen cyanide and water.

Interestingly, hydroxynitriles, once formed in competition with aminoalcohols, could also be hydrolyzed in the aqueous phase of an asteroid to form the corresponding hydroxy acids. This could be a formation pathway for hydroxy acids that are found in meteorites (Peltzer and Bada, 1978; Pizzarello et al., 2010). In our case 2-hydroxy-2-methylpropanenitrile could lead to the formation of 2-hydroxy-2-methyl-propanoic acid ($HOC(CH_3)_2COOH$). Figure 11 summarizes the thermal reactivity of ices containing $(CH_3)_2CO$, HCN, NH_3 and H_2O.

5 Conclusions

We studied the reactivity of ices containing $(CH_3)_2CO$, HCN, NH_3 and/or H_2O induced by thermal processing. No reaction was observed in HCN:$(CH_3)_2CO$ and H_2O:HCN:$(CH_3)_2CO$ ices. However, 2-hydroxy-2-methylpropanenitrile (HO-$C(CH_3)_2$-CN) was formed when NH_3:HCN:$(CH_3)_2CO$ and H_2O:NH_3:HCN:$(CH_3)_2CO$ ices were warmed, showing that HCN can only react with acetone if it has been activated by NH_3 through the formation of a stable [NH_4^+ $^-$CN] salt. The reaction between NH_3 and acetone leading to 2-aminopropan-2-ol (H_2N-$C(CH_3)_2$-OH) was not observed. This reaction is inhibited by the formation of 2-hydroxy-2-methylpropanenitrile that, according to chemical calculations, has an activation energy associated with the rate determining step of about 51 kJ mol^{-1}. Implications for astrochemistry are that it is unlikely to form precursors of 2-aminoisobutyric acid ($NH_2C(CH_3)_2COOH$) in astrophysical ices through the Strecker synthesis with acetone, as opposed to the cases of formaldehyde and acetaldehyde. The formation of 2-hydroxy-2-methylpropanenitrile could instead indicate a chemical pathway towards hydroxy acids after hydrolysis.

Acknowledgments

This work has been funded by the French national program "Physique Chimie du Milieu Interstellaire" (P.C.M.I, INSU), "Programme National de Planétologie" (PNP, CNRS), the "Centre National d'Etudes Spatiales" (C.N.E.S) from its exobiology program and a PhD grant from the Région Provence-Alpes-Côte d'Azur (PACA). This work was further supported by the ANR project VAHIIA (Grant ANR-12-JS08-0001-01) of the French Agence Nationale de la Recherche.

Notes and references

[a] *Aix-Marseille Université, CNRS, PIIM, UMR 7345, 13013 Marseille, France. E-mail: gregoire.danger@univ-amu.fr*
[b] *Departament de Química, Universitat Autònoma de Barcelona, 08193, Bellaterra, Spain. E-mail: albert.rimola@uab.cat*

Becke A. D. (1993) A new mixing of Hartree--Fock and local density-functional theories. *J. Chem. Phys.* **98**, 1372–1377.

Bernstein M. P., Sandford S. A. and Allamandola L. J. (1997) The infrared spectra of nitriles and related compounds frozen in Ar and H2O. *Astrophys. J.* **476**, 932–942.

Bockelée-Morvan D., Crovisier J., Mumma M. J. and Weaver H. A. (2004) The composition of cometary volatiles. *Comets II*, 391–424. Available at: http://www.lesia.obspm.fr/perso/jacques-crovisier/biblio/preprint/boc04_comets2.pdf.

Boonman A. M. S., Stark R., van der Tak F. F. S., van Dishoeck E. F., van der Wal P. B., Schäfer F., de Lange G. and Laauwen W. M. (2001) Highly abundant HCN in the inner envelope of GL 2591: Probing the birth of a hot core? *Astrophys. J.* **553**, L63–L67.

Bossa J. B., Duvernay F., Theulé P., Borget F., D'Hendecourt L. and Chiavassa T. (2009) Methylammonium methylcarbamate thermal formation in interstellar ice analogs: a glycine salt precursor in protostellar environments. *Astron. Astrophys.* **506**, 601–608.

Bossa J. B., Theulé P., Duvernay F. and Chiavassa T. (2009) NH2CH2OH thermal formation in interstellar ices contribution to the 5-8 μm region toward embedded protostars. *Astrophys. J.* **707**, 1524–1532. Available at: http://stacks.iop.org/0004-637X/707/i=2/a=1524?key=crossref.76b3d72cf56a7c9166c954ec2ea35759 [Accessed December 2, 2014].

Bouilloud M., Fray N., Benilan Y., Cottin H., Gazeau M.-C. and Jolly a. (2015) Bibliographic review and new measurements of the infrared band strengths of pure molecules at 25 K: H2O, CO2, CO, CH4, NH3, CH3OH, HCOOH and H2CO. *Mon. Not. R. Astron. Soc.* **451**, 2145–2160. Available at: http://mnras.oxfordjournals.org/cgi/doi/10.1093/mnras/stv1021.

Burton A. S., Glavin D. P., Elsila J. E., Dworkin J. P., Jenniskens P. and Yin Q.-Z. (2014) The amino acid composition of the Sutter's Mill CM2 carbonaceous chondrite. *Meteorit. Planet. Sci.* **49**, 2074–2086. Available at: http://doi.wiley.com/10.1111/maps.12281 [Accessed December 3, 2014].

Cheung A. C., Rank D. M., Townes C. H., Thornton D. D. and Welch W. J. (1968) Detection of NH3 molecules in the interstellar medium by their microwave emission. *Phys. Rev. Lett.* **21**, 1701–1705.

Civalleri B., Zicovich-Wilson C. M., Valenzano L. and Ugliengo P. (2008) B3LYP augmented with an empirical dispersion term (B3LYP-D*) as applied to molecular crystals. *CrystEngComm*.

Combes F., Gerin M., Wootten A., Wlodarczak G., Clausset F. and Encrenaz P. J. (1987) Acetone in interstellar space. *Astron. Astrophys.* **180**, L13–L16.

Cronin J. R. and Moore C. B. (1971) Amino Acid analyses of the murchison, murray, and allende carbonaceous chondrites. *Science* **172**, 1327–1329.

Crovisier J. and Bockelée-Morvan D. (1999) Remote Observations of the Composition of Cometary Volatiles. *Space Sci. Rev.* **90**, 19–32. Available at: http://adsabs.harvard.edu/abs/1999SSRv...90...19C.

Danger G., Borget F., Chomat M., Duvernay F., Theulé P., Guillemin J. C., Le Sergeant d'Hendecourt L. and Chiavassa T. (2011) Experimental investigation of aminoacetonitrile formation through the Strecker synthesis in astrophysical-like conditions: reactivity of methanimine (CH2NH), ammonia (NH3), and hydrogen cyanide (HCN). *Astron. Astrophys.* **535**, A47. Available at: <Go to ISI>://000297841200059.

Danger G., Duvernay F., Theulé P., Borget F. and Chiavassa T. (2012) Hydroxyacetonitrile (HOCH2CN) Formation in Astrophysical Conditions. Competition With the Aminomethanol, a Glycine Precursor. *Astrophys. J.* **756**, 11. Available at: http://stacks.iop.org/0004-637X/756/i=1/a=11?key=crossref.11b951a95096495dd9b1c863f46601d0 [Accessed December 1, 2014].

Danger G., Rimola A., Abou Mrad N., Duvernay F., Roussin G., Theulé P. and Chiavassa T. (2014) Formation of hydroxyacetonitrile (HOCH2CN) and polyoxymethylene (POM)-derivatives in comets from formaldehyde (CH2O) and hydrogen cyanide (HCN) activated by water. *Phys. Chem. Chem. Phys.* **16**, 3360–70. Available at: http://www.ncbi.nlm.nih.gov/pubmed/24202268 [Accessed November 25, 2014].

Dovesi R., Saunders V. R., Roetti C., Orlando R., Zicovich-Wilson C. M., Pascale F., Civalleri B., Doll K., Harrison N. M., Bush I. J., D'Arco P. and Llunell M. (2009) CRYSTAL09 User's Manual. *Univ. Torino*.

Duvernay F., Dufauret V., Danger G., Theulé P., Borget F. and Chiavassa T. (2010) Chiral molecule formation in interstellar ice analogs: alpha-aminoethanol NH2CH(CH3)OH. *Astron. Astrophys.* **523**, A79. Available at: <Go to ISI>://000285346600082.

Ehrenfreund P. and Charnley S. B. (2000) Organic molecules in the interstellar medium, comets and meteorites: A Voyage from Dark Clouds to the Early Earth. *Annu. Rev. Astron. Astrophys.* **38**, 427–483. Available at: http://arjournals.annualreviews.org/doi/abs/10.1146/annurev.astro.38.1.427.

Elsila J. E., Glavin D. P. and Dworkin J. P. (2009) Cometary glycine detected in samples returned by Stardust. *Meteorit. Planet. Sci.* **44**, 1323–1330.

Engel M. H. and Macko S. A. (1997) Isotopic evidence for extraterrestrial non-racemic amino acids in the Murchison meteorite. *Nature* **389**, 265–268.

Fresneau A., Danger G., Rimola A., Duvernay F., Theulé P. and Chiavassa T. (2015) Ice chemistry of acetaldehyde reveals competitive reaction in Strecker synthesis of alanine: formation of HO-CH(CH3)-NH2 vs. HO-CH(CH3)-CN. *Mon. Not. R. Astron. Soc.* **451**, 1649–1660.

Fresneau A., Danger G., Rimola A., Theulé P., Duvernay F. and Chiavassa T. (2014) Trapping in water - an important prerequisite for complex reactivity in astrophysical ices: the case of acetone (CH3)2C = O and ammonia NH3. *Mon. Not. R. Astron. Soc.* **443**, 2991–3000. Available at: http://mnras.oxfordjournals.org/cgi/doi/10.1093/mnras/stu1353 [Accessed November 25, 2014].

Friedel D. N., Snyder L. E., Remijan A. J. and Turner B. E. (2005) Detection of interstellar acetone toward the Orion-KL hot core. *Astrophys. J.* **632**, L95–L98.

Frisch M. J., Trucks G. W., Schlegel H. B., Scuseria G. E., Robb M. A., Cheeseman J. R., Scalmani G., Barone V., Mennucci B., Petersson G. A., Nakatsuji H., Caricato M., Li X., Hratchian H. P., Izmaylov A. F., Bloino J., Zheng G., Sonnenberg J. L., Hada M., Ehara M., Toyota K., Fukuda R., Hasegawa J., Ishida M., Nakajima T., Honda Y., Kitao O., Nakai H., Vreven T., J. A. Montgomery J., Peralta J. E., Ogliaro F., Bearpark M., Heyd J. J., Brothers E., Kudin K. N., Staroverov V. N., Keith T., Kobayashi R., Raghavachari J. N., Rendell K. A., Burant J. C., Iyengar S. S., Tomasi J., Cossi M., Rega N., Millam J. M., M. Klene J. E. K., Cross J. B., Bakken V., Adamo C., Jaramillo J., Gomperts R., Stratmann R. E., Yazyev O., Austin A. J., Cammi R., Pomelli C., Ochterski J. W., Martin R. L., K. Morokuma V. G. Z., Voth G. A.,

Salvador P., Dannenberg J. J., Dapprich S., Daniels A. D., Farkas O., Foresman J. B., Ortiz J. V., Cioslowski J. and Fox D. J. (2013) *GUASSIAN 09*., Gaussian Inc., Wallingford CT.

Gerakines P. a., Moore M. H. and Hudson R. L. (2004) Ultraviolet photolysis and proton irradiation of astrophysical ice analogs containing hydrogen cyanide. *Icarus* **170**, 202–213. Available at: http://linkinghub.elsevier.com/retrieve/pii/S0019103504000685 [Accessed November 25, 2014].

Gerakines P. A., Schutte W. A., Greenberg J. M. and van Dishoeck E. F. (1995) The infrared band strengths of H2O, CO and CO2 in laboratory simulations of astrophysical ice mixtures. *Astron. Astrophys.* **296**, 810–818.

Glavin D. P., Callahan M. P., Dworkin J. P. and Elsila J. E. (2010) The effects of parent body processes on amino acids in carbonaceous chondrites. *Meteorit. Planet. Sci.* **45**, 1948–1972. Available at: http://doi.wiley.com/10.1111/j.1945-5100.2010.01132.x [Accessed December 2, 2014].

Grimme S. (2006) Semiempirical GGA-type density functional constructed with a long-range dispersion correction. *J. Comput. Chem.* **27**, 1787–1799.

Grimme S., Antony J., Ehrlich S. and Krieg H. (2010) A consistent and accurate ab initio parametrization of density functional dispersion correction (DFT-D) for the 94 elements H-Pu. *J. Chem. Phys.* **132**.

Le Guillou C., Bernard S., Brearley A. J. and Remusat L. (2014) Evolution of organic matter in Orgueil, Murchison and Renazzo during parent body aqueous alteration: In situ investigations. *Geochim. Cosmochim. Acta* **131**, 368–392. Available at: http://linkinghub.elsevier.com/retrieve/pii/S0016703713006595 [Accessed December 2, 2014].

Herbst E. and van Dishoeck E. F. (2009) Complex Organic Interstellar Molecules. *Annu. Rev. Astron. Astrophys.* **47**, 427–480.

Kerkhof O., Schutte W. A. and Ehrenfreund P. (1999) The infrared band strengths of CH3OH , NH3 and CH4 in laboratory simulations of astrophysical ice mixtures. *Astron. Astrophys.* **346**, 990–994.

Kvenvolden K., Lawless J., Pering K., Peterson E., Flores J., Ponnamperuma C., Kaplan I. R. and Moore C. (1970) Evidence for extraterrestrial amino-acids and hydrocarbons in the Murchison meteorite. *Nature* **228**, 923–926. Available at: http://www.nature.com/nature/journal/v228/n5275/abs/228923a0.html [Accessed December 3, 2014].

Lara L.-M., Rodrigo R., Tozzi G. . P., Boehnhardt H. and Leisy P. (2004) The gas and dust coma of Comet C/1999 H1 (Lee)*. *Astron. Astrophys.* **420**, 371–382.

Lee C., Yang W. and Parr R. G. (1988) Development of the Colle-Salvetti correlation-energy formula into a functional of the electron density. *Phys. Rev. B* **37**, 785–789.

Martins Z., Alexander C. M. O., Orzechowska G. E., Fogel M. L. and Ehrenfreund P. (2007) Indigenous amino acids in primitive CR meteorites. *Meteorit. Planet. Sci.* **42**, 2125–2136.

McQuarrie D. (1986) *Statistical Mechanics*., Harper and Row, New York.

Merrick J. P., Moran D. and Radom L. (2007) An evaluation of harmonic vibrational frequency scale factors. *J. Phys. Chem. A* **111**, 11683–11700.

Mispelaer F., Theulé P., Aouididi H., Noble J. A., Duvernay F., Danger G., Roubin P., Morata O., Hasegawa T. and Chiavassa T. (2013) Diffusion measurements of CO, HNCO, H2CO, and NH3 in amorphous water ice. *Astron. Astrophys.* **555**, 1–11.

Noble J. A., Theulé P., Borget F., Danger G., Chomat M., Duvernay F., Mispelaer F. and Chiavassa T. (2013) The thermal reactivity of HCN and NH3 in interstellar ice analogues. *Mon. Not. R. Astron. Soc.* **428**, 3262–

3273. Available at: http://mnras.oxfordjournals.org/cgi/doi/10.1093/mnras/sts272 [Accessed December 2, 2014].

Peltzer E. T. and Bada J. L. (1978) Alpha-Hydroxycarboxylic acids in the Murchison meteorite. *Nature* **272**, 443–444.

Pizzarello S., Wang Y. and Chaban G. M. (2010) A comparative study of the hydroxy acids from the Murchison, GRA 95229 and LAP 02342 meteorites. *Geochim. Cosmochim. Acta* **74**, 6206–6217. Available at: http://linkinghub.elsevier.com/retrieve/pii/S0016703710004539 [Accessed December 2, 2014].

Rimola A., Sodupe M. and Ugliengo P. (2012) Computational Study of Interstellar Glycine Formation Occurring At Radical Surfaces of Water-Ice Dust Particles. *Astrophys. J.* **754**, 24.

Rimola A., Sodupe M. and Ugliengo P. (2010) Deep-space glycine formation via Strecker-type reactions activated by ice water dust mantles. A computational approach. *Phys. Chem. Chem. Phys.* **12**, 5285–5294.

Rubin A. E., Trigo-Rodríguez J. M., Huber H. and Wasson J. T. (2007) Progressive aqueous alteration of CM carbonaceous chondrites. *Geochim. Cosmochim. Acta* **71**, 2361–2382. Available at: http://linkinghub.elsevier.com/retrieve/pii/S001670370700083X [Accessed December 2, 2014].

Snyder L. E. and Buhl D. (1971) Observations of radio emission from interstellar hydrogen cyanide. *Astrophys. J.* **163**, L47–L52.

Snyder L. E., Lovas F. J., Mehringer D. M., Yanti Miao N., Kuan Y.-J., Hollis J. M. and Jewell P. R. (2002) Confirmation of interstellar acetone. *Astrophys. J.* **578**, 245–255.

Strecker A. (1854) Ueber einen neuen aus Aldehyd-Ammoniak und Blausäure entstehenden Körper. *Ann. der Chemie und Pharm.* **91**, 349–351.

Vinogradoff V., Duvernay F., Farabet M., Danger G., Theulé P., Borget F., Guillemin J. C. and Chiavassa T. (2012) Acetaldehyde solid state reactivity at low temperature: Formation of the acetaldehyde ammonia trimer. *J. Phys. Chem. A* **116**, 2225–2233.

Vinogradoff V., Rimola A., Duvernay F., Danger G., Theulé P. and Chiavassa T. (2012) The mechanism of hexamethylenetetramine (HMT) formation in the solid state at low temperature. *Phys. Chem. Chem. Phys.* **14**, 12309–12320. Available at: http://www.ncbi.nlm.nih.gov/pubmed/22850541 [Accessed December 1, 2014].